Carbohydrate Polymers 108 (2014) 183–191

Contents lists available at ScienceDirect

Carbohydrate Polymers

journal homepage: www.elsevier.com/locate/carbpol

Effect of gums on the rheological characteristics and microstructure of acid-induced SPI-gum mixed gels

Yuan-yuan Chang[a,1], Dong Li[b,1], Li-jun Wang[a,*], Chong-hao Bi[b], Benu Adhikari[c]

[a] College of Food Science and Nutritional Engineering, Beijing Key Laboratory of Functional Food from Plant Resources, China Agricultural University, P.O. Box 50, 17 Qinghua Donglu, Beijing 100083, China
[b] College of Engineering, National Energy R&D Center for Non-food Biomass, China Agricultural University, Beijing, China
[c] School of Applied Sciences, RMIT University, City Campus, Melbourne, VIC 3001, Australia

ARTICLE INFO

Article history:
Received 28 December 2013
Received in revised form 19 February 2014
Accepted 28 February 2014
Available online 12 March 2014

Keywords:
Xanthan gum
Guar gum
Rheological properties
Microstructure
Burger model
Soy protein isolate

ABSTRACT

The effect of addition of xanthan gum (XG) and guar gum (GG) on the rheological properties and microstructure of glucono-δ-lactone induced soy protein isolate (SPI)-XG gels and SPI-GG gels was investigated using steady and dynamic rheological tests, creep-recovery and confocal laser scanning microscopy (CLSM). Results showed that the apparent viscosity of SPI-gum (XG, GG) mixed solutions increased with the increase in the gum (XG, GG) concentration. The storage (G') and loss (G'') moduli of SPI-gum (XG, GG) mixed gels increased in the presence and increase in the gum (XG, GG) concentration. The Burger's model fitted the creep recovery data well ($R^2 > 0.919$) and showed that both the instantaneous and equilibrium (retarded) elastic components of this model increased with the increase in SPI and gum concentrations. The proportion occupied by gum in mixed gels was found to increase with the increase in the concentration of gums which increased the density of protein aggregates in the mixed gels.

1. Introduction

Proteins and polysaccharides are important in imparting unique texture and taste in food products. It has been commonly accepted that proteins and polysaccharides interact with each other when they are brought together (Corredig, Sharafbafi & Kristo, 2011; de Kruif & Tuinier, 2001; Ye, Hemar & Singh, 2004). Protein–polysaccharide complexes show quite different characteristics compared to the protein and polysaccharide involved (Perez, Carrara, Sánchez, Santiago & Rodríguez Patino, 2009). The protein–polysaccharide interaction can be judiciously utilized to design and formulation of new food products (Alvarez, Fernández, Olivares & Canet, 2012; Perez et al., 2009). Hence, better understanding of protein–polysaccharide interaction is very important for developing new products in food industry.

Soy protein isolate (SPI) contains higher than 90% soy protein and is mainly comprised of glycinin (11S) and β-conglycinin (7S) (Petruccelli & Anon, 1995). SPI has unique functional properties such as gelling, foaming, emulsifying, water-holding and fat-absorption and is nutritionally rich; hence, it is widely used in food industry (Bi, Li, Wang, Wang & Adhikari, 2013; Wong & Kitts, 2003). In addition, the acid-induced gelation of SPI is important in food processing, for example, in producing sausages. The SPI is often used in a number of food formulations as an important food ingredient (Morr, 1990).

The lowering of pH to the isoelectric point of protein such as SPI greatly reduces the electrostatic repulsion between the protein molecules which helps the formation of gels. Glucono-δ-lactone (GDL) is a widely used acid curing agent, which does not precipitate protein. The precipitation of protein can only occur when the GDL breaks down into glucose acid and subsequently reduces the pH to the isoelectric point of a protein (Cavallieri & Da Cunha, 2008).

Xanthan gum (XG) is a high molecular weight polysaccharide with low negative charge and comes from microbial source (Whitcomb, EK & Macosko, 1977). Guar gum (GG) is a cold water soluble and uncharged polysaccharide extracted from endosperm of guar beans (Roberts, 2011). XG and GG are natural food gums with unique functional characteristics; hence, they are often used in food, pharmaceutical and other industries as emulsifiers, stabilizers and foaming agents (Andrew, 1977; Ye et al., 2004).

The rheological properties and microstructure of protein–polysaccharide complexes can influence the choice of manufacturing method used and the sensorial characteristics

* Corresponding author. Tel.: +86 10 62737351; fax: +86 10 62737351.
E-mail address: wlj@cau.edu.cn (L.-j. Wang).
[1] These authors contributed equally to this work.

http://dx.doi.org/10.1016/j.carbpol.2014.02.089
0144-8617/

Nomenclature

η	apparent viscosity (Pa s)
γ	shear rate (1/s)
K	consistency index (Pa s^n)
n	flow behavior index (dimensionless)
K'	power law constant (Pa s^n)
K''	power law constant (Pa s^n)
n'	frequency exponent (dimensionless)
n''	frequency exponent (dimensionless)
ω	angular frequency
E_1	instantaneous elastic parameter (Pa)
E_2	retarded elastic parameter (Pa)
η_1	coefficient of viscosity associated with viscosity flow (Pa s)
t_2	retardation time (s)
σ	constantly applied compressive stress (Pa)

of final products. In this context, a number of studies have been undertaken to quantify and elucidate the effect of addition of polysaccharides on microstructure, foaming, emulsifying, rheological properties and water holding properties of protein (Joshi, Aldred, Panozzo, Kasapis & Adhikari, 2014; Kasran, Cui & Goff, 2013; Wang, Li, Wang & Adhikari, 2011; Zhu, Yang, Ahmad, Li, Wang & Liu, 2008). Most of these studies used carrageenan or pectin as model polysaccharides. Joshi et al. (2014) studied the complexation between lentil protein and lentil starch. To our knowledge there are no studies on the effect of gums (xanthan gum, guar gum) on the rheological behavior and microstructure of GDL induced SPI-gum mixed gels.

The objective of this study was to quantify and elucidate the effect of addition of XG and GG′s in varying concentration on the rheological properties and microstructure of GDL induced SPI-gum gels. The concentrations of XG, GG and SPI were varied from 0.02 to 0.2% (w/w), 0.05–0.3% (w/w) and 4–8% (w/w), respectively. The results from this study provide better understanding of SPI-gum complexes and allow better control of these complexes in manufactured foods.

2. Materials and methods

2.1. Materials

Soy protein isolate (containing 92.8% protein) was purchased from Beijing Messenger Biotechnology Co. Ltd (Beijing, China). The glucono-δ-lactone (GDL) was purchased from Tianjin Fuchen Technology Ltd (Tianjin, China). Xanthan gum was purchased from Zibo Zhongxuan Biotechnology Co. Ltd (Beijing, China). Guar gum was purchased from Henan Jialian Biotechnology Co. Ltd (Henan, China). Rhodamine B (BS) was purchased from Beijing Yinghai fine chemical industry (Beijing, China). These materials were used without further purification.

2.2. Sample preparation

2.2.1. Preparation of SPI-gum (XG, GG) solutions

The SPI was dissolved in deionized water at 25 °C for 2 h using a magnetic stirrer. The stock solutions containing 9% (w/w) and 12% (w/w) SPI concentrations were prepared. The SPI stock solutions were heated to 95 °C in a water bath for 30 min to fully denature the protein. These solutions were stored in 4 °C refrigerator overnight after cooling to 25 °C. The XG and GG were dissolved in deionized water separately at 25 °C for 2 h using a magnetic stirrer in order to prepare 1% (w/w) stock solutions of XG and GG. The XG stock solution was thoroughly blended with SPI stock solution to prepare SPI (4%, 6% and 8%, w/w)-XG (0%, 0.02%, 0.05%, 0.1% and 0.2%, w/w) blends. SPI (4%, 6% and 8%, w/w)-GG (0%, 0.05%, 0.1%, 0.2% and 0.3%, w/w) blends were also prepared following the same procedure. These blends were stored overnight in a refrigerator maintained at 4 °C.

2.2.2. Preparation of acid induced SPI-gum (XG, GG) gels

The GDL was added to the blends as soon as they were taken out from the refrigerator with a continuous and gentle shaking. The final concentration of GDL in every sample was maintained at 1.5% (w/w).

2.3. Rheological tests

Rheological tests were performed using AR2000ex rheometer (TA Instruments Ltd., Crawley, UK) with aluminum parallel plate geometry (40 mm diameter, 1 mm gap). A thin layer of silicone oil was added on the edge of the sample to avoid evaporation. The linear viscoelastic region of each sample was determined by strain sweep tests at 1 Hz (data not shown). All the tests were carried out allowing the sample to equilibrate for 2 min to eliminate the effect of loading of the sample on the plate. The temperature of the sample was controlled using a Peltier system connected with a water bath.

Rheological tests included steady shear, time sweep, frequency sweep and creep-recovery and were carried out according to Wang et al. (Wang, Wang, Li, Xue & Mao, 2009) with a slight modification.

2.3.1. Rheological tests for the complexed samples

2.3.1.1. Steady shear test. The steady shear test was performed at 20 °C over the shear rate range of 1–100 s^{-1} (Steffe, 1996). The variations of apparent viscosity with shear rate were measured in these tests.

2.3.2. Dynamic rheological tests of complexed gels

2.3.2.1. Time sweep test. The time sweep tests were executed at 60 °C and at a constant frequency of 1 Hz and the storage modulus (G') and loss modulus (G'') were recorded. Based on the strain sweep tests the strain amplitude of time sweep test was selected to be 1% to keep the strain amplitude of all samples in the linear viscoelastic region.

2.3.2.2. Frequency sweep test. The frequency sweep test was carried out at 20 °C over the angular frequency range of 0.1–10 rad/s. In order to keep the strain amplitude in the linear viscoelastic region for all samples, the strain amplitude for frequency sweep test was chosen to be 1%.

2.3.2.3. Creep-recovery test. Creep-recovery tests were carried out under the shear stress of 7.985 Pa at 20 °C. In creep-recovery test, the stress response of samples under constant stress in a time frame of 3 min was measured. This stress was subsequently removed and the response of samples was recorded for another 3 min.

The effect of gum concentration on the creep-recovery characteristics data of protein–polysaccharide complex gel were represented by using the Berger's model equation (Wang et al., 2009).

2.4. Confocal laser scanning microscopy (CLSM)

The SPI-gum (XG, GG) mixed gels were prepared as described in Section 2.2 above. The gels were stained with an aqueous solution of Rhodamine B (BS) prior to gelation (1 mL of a sample +10 μL of a 0.1% (w/w) Rhodamine B) and then allowed to gel (60 °C water bath for 30 min) in a concave slip covered with a slide and hermetically sealed to prevent evaporation (Bi, Li, Wang & Adhikari,

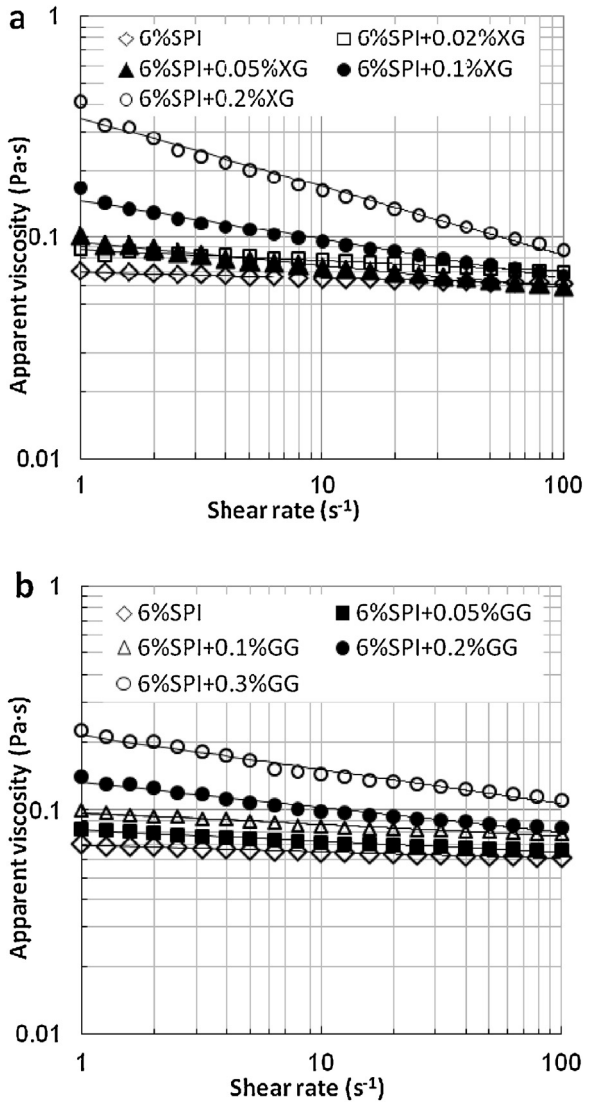

Fig. 1. (a) Variation of apparent viscosity of SPI-XG solutions as a function of shear rate at 20 °C. (b) Variation of apparent viscosity of SPI-GG solutions as a function of shear rate at 20 °C.

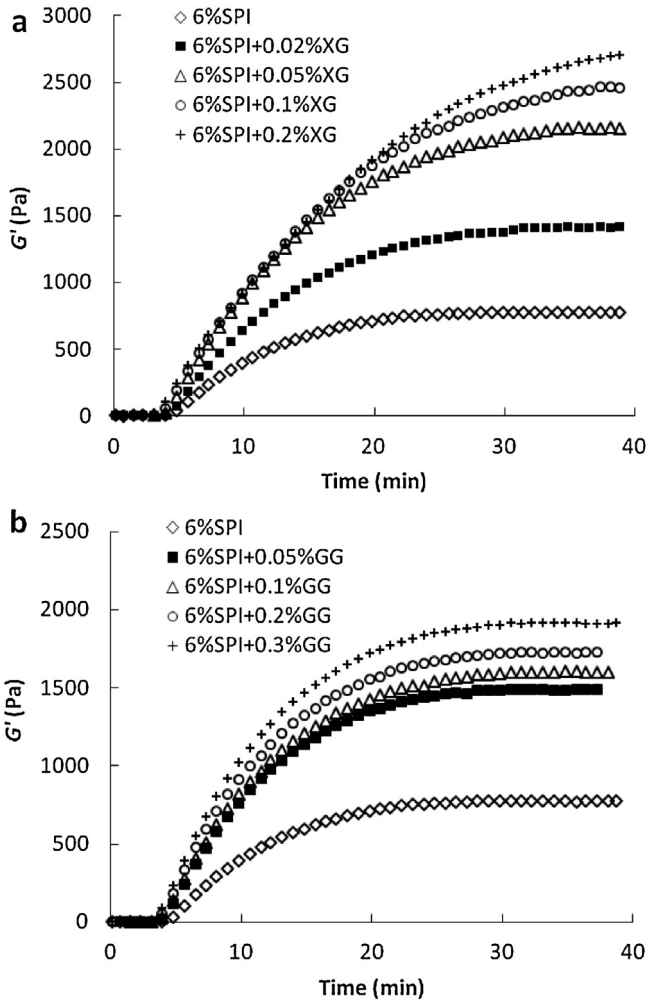

Fig. 2. (a) Variation of storage modulus, G' with time of 6% (w/w) SPI gel and SPI-XG gels at 60 °C. (b) Variation of storage modulus, G' with time of 6% (w/w) SPI gel and SPI-GG gels at 60 °C.

2013). All the samples were investigated using Leica TCS SP5 confocal laser scanning microscope (CLSM) equipped with a DMI6000 inverted 146 microscope (Leica Microsystems GmbH, Mannheim, Germany). The objective lens used was a 40×/NA 0.85 HC PL APO. The excitation wavelength was 543 nm (He/Ne laser) and the emission was recorded between 600 nm and 680 nm. Digital images were acquired in 1024 × 1024 pixel resolution.

2.5. Theory

2.5.1. Steady shear test

The variation of apparent viscosity of SPI and SPI-XG solutions with shear rate can be described using Power Law model (Eq. (1)), given below.

$$\eta = K \cdot \gamma^{n-1} \tag{1}$$

where η is the apparent viscosity (Pa s), γ is the shear rate (1/s), K is consistency index (Pa s^n), and n is the flow behavior index (dimensionless).

2.5.2. Frequency sweep test

The variation of G' and G'' with angular frequency of protein–polysaccharide gels can be expressed using Power Law type equations (Eqs. (2) and (3)), given below.

$$G' = K' \cdot \omega^{n'} \tag{2}$$

$$G'' = K'' \cdot \omega^{n''} \tag{3}$$

where K' and K'' are power law constants, n' and n'' are frequency exponents, ω is the angular frequency. The values of n' and n'' represent the extent of frequency dependence of the elastic modulus and provide useful information regarding the viscoelastic nature of food materials (Özkan, Xin & Chen, 2002).

2.5.3. Creep-recovery test

Creep-recovery behavior can be adequately represented by using a four element Burger's model (Ai-min, Wang, Li & Adhikari, 2012) consisting of springs and dashpots in the form of Maxwell and Kelvin components. The total strain ε is given by Eq. (4).

$$\varepsilon = \frac{\sigma}{E_1} + \frac{\sigma}{E_2}\left[1 - \exp\left(-\frac{t}{t_2}\right)\right] + \frac{\sigma}{n_1}t \tag{4}$$

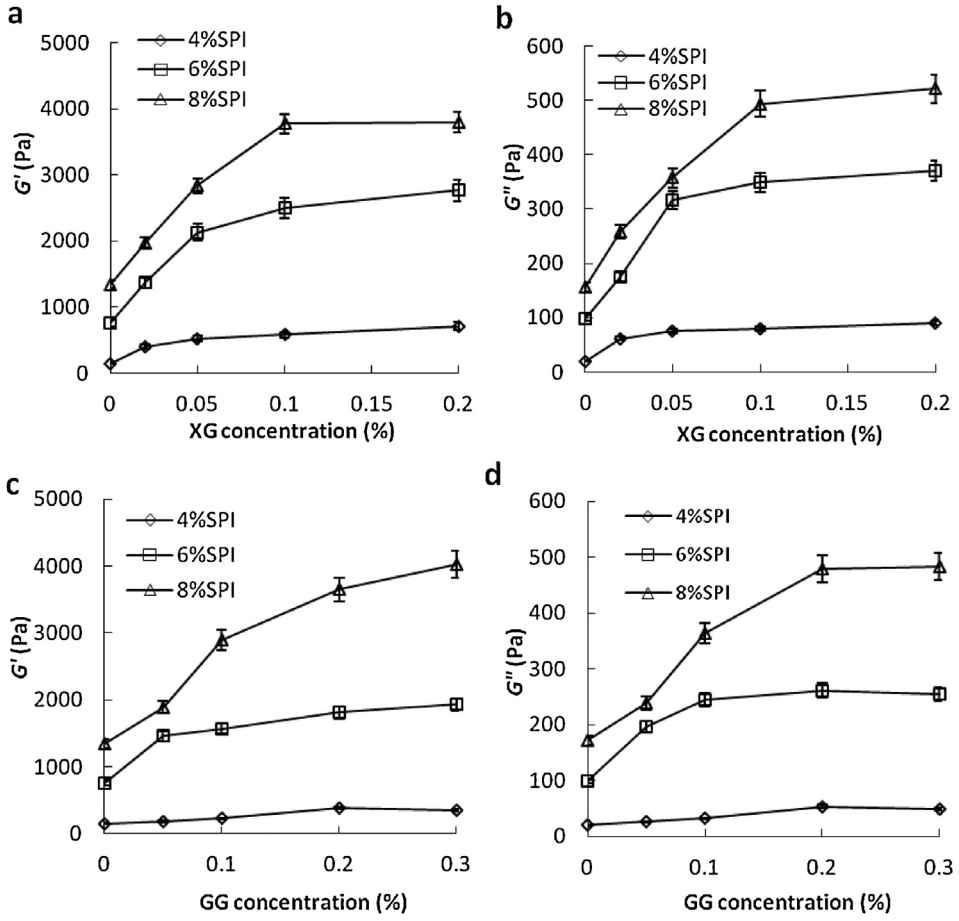

Fig. 3. The effect of gum (XG, GG) and SPI concentrations on the storage (G') and loss (G'') moduli of SPI-gum (XG, GG) gels at 20 °C.

where E_1 (Pa) is the instantaneous elastic parameter, E_2 (Pa) is the retarded elastic parameter, η_1 (Pa s) is the viscous parameter associated with viscous flow, t_2 is the retardation time, and σ (Pa) is the applied compressive stress. The parameters E_1, E_2, η_1 and t_2 can be obtained from fitting Eq. (4) to experimental creep recovery data.

The recovery rate (%) was used to calculate the percentage recovery of SPI-gum (XG, GG) subjected to a certain strain as given by Eq. (5).

$$\text{Recovery}\,(\%) = \frac{\text{maxium strain} - \text{final strain}}{\text{maxium strain}} \times 100\% \quad (5)$$

2.6. Statistical analysis

All rheological measurements were carried out in triplicate. The rheological experimental data were directly obtained from TA Rheology Advantage Data Analysis software V 5.4.7 (TA Instruments Ltd., New Castle, USA). The average value of the three runs was reported as the measured value ± standard deviation.

The steady state shear data and frequency sweep data were analyzed in SPSS 21.0 (SPSS Inc., Chicago, USA). The creep data were modeled according to Berger's model, using the non-linear regression feature in SPSS 21.0 (SPSS Inc., Chicago, USA). The significant difference between sample means was evaluated by analysis of variance (ANOVA), the confidence level was set at 95% ($p < 0.05$).

3. Results and discussion

3.1. Rheological characteristics of mixed solutions rheological tests

3.1.1. Steady state shear characteristics

Fig. 1(a) presents the steady shear flow curves of SPI-XG mixed solutions at different shear rates. The apparent viscosity of samples has increased with the increase in concentration of XG. The apparent viscosity of all samples decreased with the increase in the shear rate indicating to a shear thinning behavior. XG is a large molecule having large molecular weight and it is expected for this gum to increase the apparent viscosity with increase in concentration (Xu, Xu, Liu, Chen & Gong, 2013). The shear thinning behavior is related to the arrangement of molecular structure along the stream line of shear flow (Chagas, Machado, Haag, De Souza & Lucas, 2004). Molecular network cannot be significantly altered at low shear rates and unaltered molecular network offers increased resistance to shear deformation; hence, the protein–gum mixed system shows higher apparent viscosity values at low shear rates. At the high shear rates, the molecular network is destroyed and the dispersed molecules arrange themselves along the shear flow direction, which greatly decreases the resistance to shearing motion and hence decreases the apparent viscosity (Oh, So & Yang, 1999; Xu et al., 2013). The shear thinning behavior of SPI-XG solutions observed in this figure is in accordance with the earlier publications which reported that that protein–gum mixed solution, such as SPI-flaxseed gum exhibited shear-thinning behavior (Bi, Li,

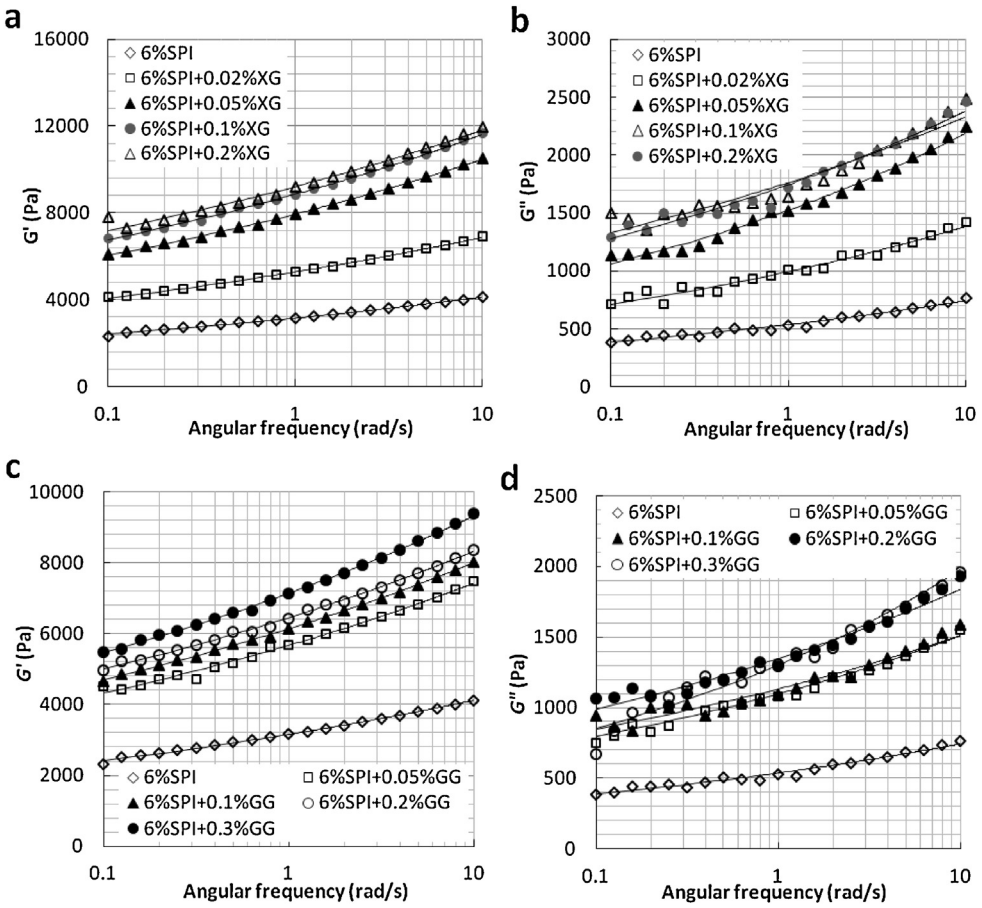

Fig. 4. The storage (G') and loss (G'') moduli of SPI-gum (XG, GG) gels and 6% SPI gels at 20 °C as a function of angular frequency.

Wang, Wang, et al., 2013). It can also be seen from Fig. 1(b) that the trend of apparent viscosity in SPI-GG system is similar to that in SPI-XG system.

3.2. Dynamic rheological behavior of mixed gels

3.2.1. Time sweep

Time sweep curves of SPI (6%, w/w)–XG (0–0.2%, w/w) gels are shown in Fig. 2(a). As can be seen from this figure, these formulations are capable of producing gel network even in the absence of XG. The time sweep data also show that the strength of these gels increases until the respective maximum gel strength is reached. This is because the slow breakdown of GDL gradually decreases the pH of the system (Cavallieri & Da Cunha, 2008). The gel strength of system reaches its peak value when the pH value of the system reaches the isoelectric point of SPI (pH = 4.8). It can also be seen from Fig. 2(b) that the trend of the time sweep curves of SPI-GG system is similar to that of SPI-XG system. The storage modulus (G') of SPI-XG gels was found to be much higher than that of SPI-GG gels. This may be due to much higher viscosity of XG than that

Table 1
The effect of XG concentration and SPI concentration on parameters (K', K'', n' and n'') of the SPI-XG gels.

SPI concentration (%)	XG concentration (%)	$G' = K' \cdot \omega^{n'}$			$G'' = K'' \cdot \omega^{n''}$		
		K'(Pa s^n)	n'	R^2	K'' (Pa s^n)	n''	R^2
4	0	688.8 ± 23.8^d	0.1127 ± 0.00184^b	0.998	133.2 ± 5.05^c	0.1518 ± 0.00792^a	0.981
	0.02	1591 ± 128.7^c	0.1231 ± 0.00078^a	0.991	321 ± 15.23^b	0.1645 ± 0.00417^a	0.967
	0.05	2044.4 ± 126.7^b	0.1141 ± 0.0058^b	0.998	388.7 ± 13.16^a	0.1534 ± 0.00318^a	0.978
	0.10	2090.5 ± 46.0^b	0.1081 ± 0.00071^b	0.997	398.9 ± 22.69^a	0.1224 ± 0.00339^b	0.950
	0.20	2555.2 ± 60.6^a	0.0979 ± 0.00467^c	0.995	405.4 ± 8.47^a	0.1275 ± 0.00410^b	0.986
6	0	3153.2 ± 63.2^d	0.1158 ± 0.000354^b	0.995	536.2 ± 77.4^d	0.1417 ± 0.0021^{ab}	0.976
	0.02	5280.6 ± 283.3^c	0.1142 ± 0.00236^b	0.999	993.8 ± 50.1^c	0.1437 ± 0.0103^{ab}	0.960
	0.05	7952.1 ± 119.4^b	0.1195 ± 0.00230^a	0.999	1525.3 ± 96.7^b	0.1572 ± 0.0073^a	0.986
	0.10	8860.7 ± 55.8^a	0.1174 ± 0.00190^{ab}	0.999	1763.7 ± 158.5^a	0.1215 ± 0.0181^d	0.932
	0.20	9216.1 ± 302.4^a	0.1074 ± 0.00184^c	0.983	1744.3 ± 71.2^a	0.1355 ± 0.0059^{bc}	0.972
8	0	4652 ± 124.9^d	0.1129 ± 0.00283^b	0.998	931.3 ± 108.23^d	0.1423 ± 0.00049^a	0.960
	0.02	6424.6 ± 216.8^c	0.1162 ± 0.00205^b	0.990	1539.2 ± 153.02^c	0.1548 ± 0.00679^a	0.966
	0.05	9534 ± 25.7^b	0.1176 ± 0.0012^b	0.998	2481.4 ± 59.39^b	0.1600 ± 0.00120^a	0.992
	0.10	11,297 ± 234.6^a	0.1210 ± 0.00462^a	0.987	2821.2 ± 57.98^{ab}	0.1581 ± 0.00205^a	0.997
	0.20	12,346.3 ± 648.1^a	0.1224 ± 0.00106^a	0.981	3087.9 ± 271.37^a	0.1429 ± 0.02588^a	0.953

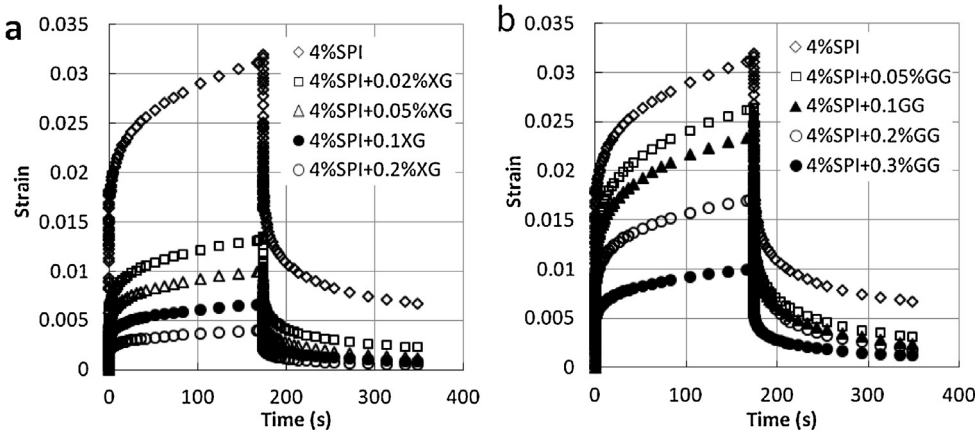

Fig. 5. (a) The effect of XG concentration on the creep-recovery of 4% SPI gel and SPI-XG gels. (b) The effect of GG concentration on the creep-recovery of 4% SPI gel and SPI-GG gels.

of GG at the same concentration and the negative charge of XG. It is reported that negatively charged polysaccharides more strongly interact with protein aggregates at the gels' pH (pH = 4.8), while a neutral polysaccharide (such as GG) does not interact with the protein aggregates (Berg, Rosenberg, van Boekel, Rosenberg & van de Velde, 2009; Whitcomb et al., 1977).

Fig. 3 shows that both the storage (G') and loss (G'') moduli increase with the increase of gum (XG, GG) concentration at any given SPI concentration. Both G' and G'' increase with the increase in SPI concentration at a given gum (XG, GG) concentration. Similar trend of increase in G' and G'' in protein–gum gels has been previously reported in the case of κ-carrageenan and soybean glycinin mixed gels (Zhu et al., 2008). These results indicate that there is strong protein–gum interaction in these GDL induced SPI-XG and SPI-GG gels and that these gel systems and such interaction produces strong gel network structure.

3.2.2. Frequency sweep

Fig. 4 presents the variation of G' and G'' as a function of angular frequency measured at 20 °C for SPI (6%, w/w)-XG (0–0.2%, w/w) and SPI (6%, w/w)-GG (0–0.3%, w/w) gels. It can be seen from this figure that both G' and G'' increase with the increase in the angular frequency. The G' and G'' values of the SPI-gum (XG, GG) gels are much higher compared to those of SPI only gel. These data indicate

Table 2
Parameters of Burger's model of SPI-gum (XG, GG) gels and recovery rate in creep-recovery test.

SPI concentration (%)	XG concentration (%)	GG concentration (%)	E_1 (Pa)	E_2 (Pa)	t_2 (s)	η_1 (KPa s)	R^2	Recovery rate (%)
	0	0	574 ± 84^{d}	969 ± 103^{d}	3.006 ± 0.465^{c}	132 ± 32.0^{d}	0.951	78.60
	0.02	0	1747 ± 185^{bc}	1866 ± 194^{c}	3.057 ± 0.226^{bc}	266 ± 36.6^{c}	0.962	82.70
4	0.05	0	2047 ± 164^{b}	2775 ± 239^{b}	3.199 ± 0.264^{bc}	374 ± 72.4^{b}	0.964	87.90
	0.1	0	3868 ± 573^{a}	3542 ± 438^{b}	3.485 ± 0.062^{b}	442 ± 54.3^{b}	0.946	88.20
	0.2	0	4357 ± 663^{a}	9006 ± 750^{a}	3.908 ± 0.152^{a}	860 ± 75.1^{a}	0.933	88.50
	0	0	2065 ± 335^{d}	3787 ± 17^{d}	3.749 ± 0.021^{a}	581 ± 23^{c}	0.971	81.70
	0.02	0	4576 ± 271^{c}	6162 ± 219^{c}	3.739 ± 0.185^{a}	947 ± 130.4^{b}	0.958	85.20
6	0.05	0	5148 ± 661^{c}	7652 ± 173^{bc}	3.833 ± 0.347^{a}	1232 ± 224^{b}	0.926	87.80
	0.1	0	8978 ± 274^{ab}	$10{,}486 \pm 228^{b}$	3.873 ± 0.208^{a}	1299 ± 152^{b}	0.952	88.40
	0.2	0	$11{,}267 \pm 921^{a}$	$14{,}068 \pm 454^{a}$	3.821 ± 0.127^{a}	2196 ± 315^{a}	0.919	88.90
	0	0	3486 ± 264^{e}	$11{,}574 \pm 684^{d}$	4.316 ± 0.223^{a}	892 ± 84^{d}	0.927	83.50
	0.02	0	4649 ± 513^{cd}	$13{,}041 \pm 993^{d}$	4.387 ± 0.025^{a}	1469 ± 237^{c}	0.944	86.60
8	0.05	0	5861 ± 416^{c}	$16{,}942 \pm 749^{c}$	4.528 ± 0.417^{a}	1682 ± 118^{bc}	0.936	88.30
	0.1	0	8690 ± 502^{b}	$20{,}476 \pm 1643^{b}$	4.241 ± 0.127^{a}	2273 ± 349^{b}	0.968	89.70
	0.2	0	$15{,}197 \pm 1230^{a}$	$27{,}475 \pm 1236^{a}$	4.382 ± 0.232^{a}	3075 ± 231^{a}	0.931	89.60
	0	0	574 ± 84^{d}	969 ± 103^{d}	3.006 ± 0.465^{b}	132 ± 32.0^{c}	0.951	78.60
	0	0.05	771 ± 93^{bc}	1041 ± 83^{d}	3.199 ± 0.264^{b}	138 ± 17.4^{c}	0.964	85.80
4	0	0.1	865 ± 51^{b}	1166 ± 14^{c}	3.395 ± 0.352^{b}	152 ± 52.0^{bc}	0.968	87.50
	0	0.2	1190 ± 194^{b}	1602 ± 121^{b}	3.570 ± 0.231^{ab}	216 ± 38.7^{b}	0.963	88.20
	0	0.3	1643 ± 95^{a}	2775 ± 185^{a}	3.939 ± 0.369^{a}	374 ± 23.9^{a}	0.964	89.80
	0	0	2065 ± 335^{e}	3787 ± 17^{e}	3.749 ± 0.021^{a}	581 ± 23^{c}	0.971	81.70
	0	0.05	3033 ± 223^{d}	4674 ± 344^{d}	3.866 ± 0.173^{a}	623 ± 85^{b}	0.942	86.90
6	0	0.1	4649 ± 713^{c}	5439 ± 627^{bc}	3.792 ± 0.235^{a}	864 ± 151^{b}	0.935	88.40
	0	0.2	6068 ± 544^{b}	6782 ± 621^{b}	3.871 ± 0.352^{a}	1175 ± 162^{a}	0.938	88.70
	0	0.3	7492 ± 477^{a}	9894 ± 863^{a}	3.910 ± 0.214^{a}	1429 ± 231^{a}	0.954	90.00
	0	0	3486 ± 264^{d}	$11{,}574 \pm 684^{d}$	4.316 ± 0.223^{a}	892 ± 84^{d}	0.927	83.50
	0	0.05	4524 ± 803^{c}	$12{,}230 \pm 326^{d}$	4.342 ± 0.148^{a}	1203 ± 105^{c}	0.936	87.60
8	0	0.1	5161 ± 632^{c}	$14{,}398 \pm 1220^{bc}$	4.295 ± 0.307^{a}	1352 ± 96^{c}	0.944	89.00
	0	0.2	7762 ± 680^{b}	$19{,}175 \pm 628^{b}$	4.590 ± 0.231^{a}	1907 ± 190^{b}	0.969	88.80
	0	0.3	$11{,}486 \pm 226^{a}$	$23{,}507 \pm 1264^{a}$	4.739 ± 0.369^{a}	2564 ± 144^{a}	0.951	91.30

that the network of mixed SPI-gum (XG, GG) gels is much stronger than the SPI only gel which corroborates with the observed microscopic structure in CLSM images (Section 3.3). These G' and G'' data also indicate that the addition of gum (XG, GG) increases the viscoelastic moduli of the SPI-gum (XG, GG) mixed gels by modifying their network structure. Besides, the G' and G'' values positively correlate with gum (XG, GG) concentration. It can also be observed from these data that $G' > G''$ in all samples implying that the solid like property in these gels is much stronger than liquid like property (Oh et al., 1999).

The effect of XG and SPI concentrations on the Power Law parameters (K', K'', n' and n'') for the SPI-XG gels is shown in Table 1. Both the G' and G'' data as a function of frequency obeyed the Power Law model ($R^2 > 0.932$). The data presented in this table suggest that the addition of XG in SPI significantly alters the dynamic rheological properties of the SPI-XG gels compared to those of SPI only gels. The magnitudes of K' and K'' of SPI-XG mixed gels are much higher than those of SPI only gels. The trend of K' and K'' in SPI-GG system is similar to that in SPI-XG system (data not shown). This observation suggests that the addition of gum (XG, GG) in SPI helps to form a stronger gel network structure.

3.2.3. Creep-recovery

The effect of XG concentration on the creep-recovery behavior of 4% SPI gel and SPI-XG mixed gels can be observed from Fig. 5(a). The deformation of the SPI-XG gels appears to decrease with the increase in XG concentration at a given SPI concentration. These creep recovery curves also show that the strain changed instantaneously in both loading and unloading processes in all the samples. The instantaneous strain of 4% (w/w) SPI only gel is the highest among all the samples. There is an instantaneous increase in strain when the stress is applied and there is an instantaneous decrease in the strain when the stress is removed. The highly stress dependent nature of strain observed in these gels can be attributed to the highly elastic nature of crosslinked gel network. These creep recovery data also suggest that XG forms stronger gel network. Similar creep recovery data of SPI–GG gels presented in Fig. 5(b) suggest that these gels also behave similar to the SPI-XG gels in terms of creep recovery. The only difference is that the SPI-GG gels are much more sensitive than the SPI-XG gels in terms of deformation.

The values of the parameters of Burger's model in the case of SPI-gum (XG, GG) mixed gels are summarized in Table 2. The Burger model fits the experimental data reasonably well ($R^2 > 0.931$). The instantaneous elastic parameter (E_1) in Berger model is smaller than the retarded elastic parameter (E_2). This observation indicates that the instantaneous elastic strain is larger than the retarded elastic and viscous flow deformation (Wu, Li, Wang, Özkan & Mao, 2010). The E_2 value reflects the magnitude of the retarded elastic deformation and the resistance to deformation caused by the three dimensional network structure of SPI-gum (XG, GG) mixed gels (Wang et al., 2009). Thus, low E_2 value in SPI only gels indicate to a simple network structure in SPI only gels. The η_1 value reflects the viscos behavior of the gels and high η_1 values indicates that the viscous component of these gels would be higher. The value of η_1 has increased with the increase in both SPI and gum (XG, GG) concentrations (Table 2). The trend of variation of viscous component in this deformation test is similar to trend of η in steady state shear flow test (Section 3.1.1). t_2 is the retardation time required for the strain of structural elements to decrease to $(1 - 1/e)$ (approximately 63%) of their maximum strain (Wu et al., 2010). The t_2 in 4% (w/w) SPI-gum (XG, GG) has increased significantly ($p < 0.05$) with the increase in gum (XG, GG) concentration. In the case of other samples, the variation in gum (XG, GG) did not alter the t_2 values significantly ($p > 0.05$) at any fixed SPI concentration.

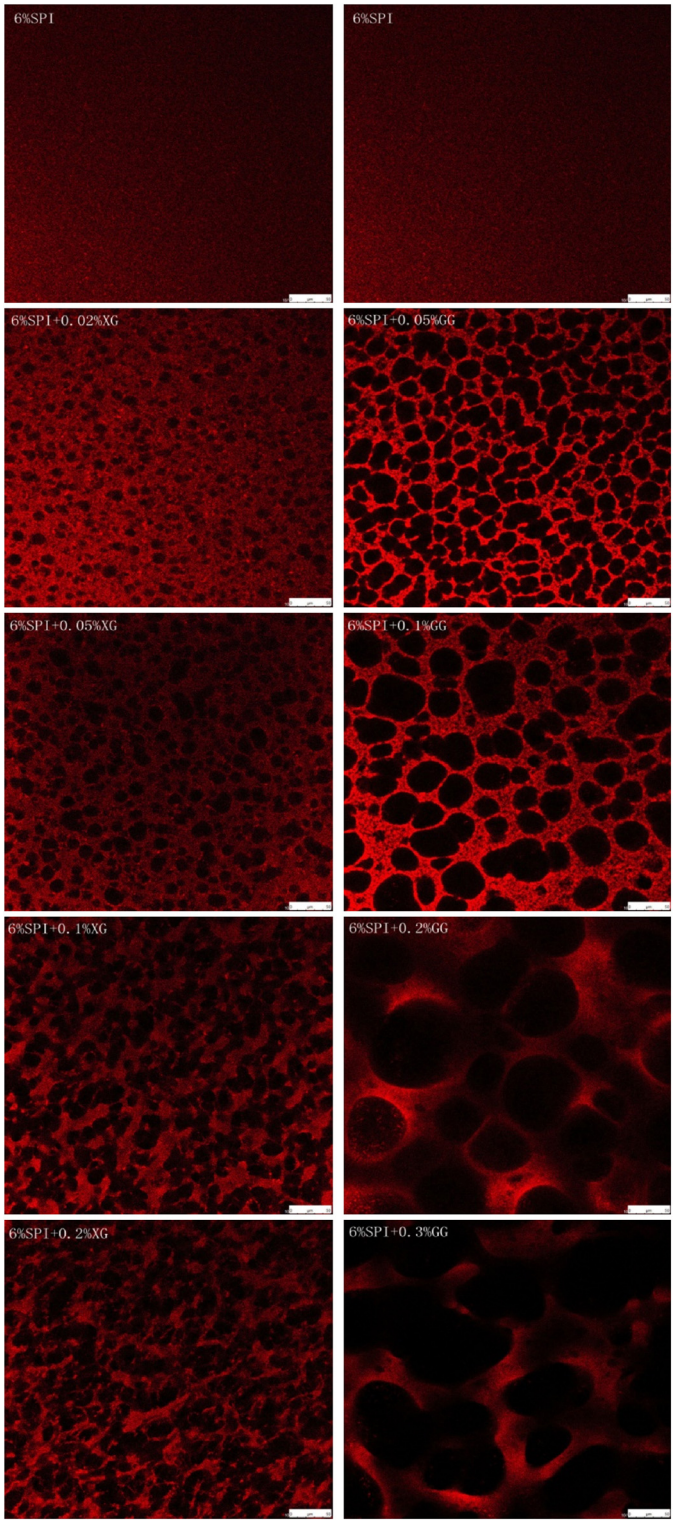

Fig. 6. CLSM images of SPI only gel, SPI-XG and SPI-GG mixed gels (the bar represents 50 μm).

The recovery data (Table 2) of all the samples show that the rate of recovery increases with the increase in SPI concentration at any given gum (XG, GG) concentration. These data also show that the rate of recovery in all samples is positively correlated with gum (XG, GG) concentration at a fixed SPI concentration. The increased recovery with increase in protein or gum concentration can be attributed to the stronger network structure at higher solid concentration.

3.3. Confocal laser scanning microscopy (CLSM)

The CLSM images of the gels are shown in Fig. 6. The protein and gum parts are depicted by bright and dark areas, respectively. As can be seen from these images, the microstructure of these gels had different degree of coarseness. The presence of gum (XG, GG) affected the microstructure of SPI quite remarkably. The microstructure of SPI only gel appears to be much more homogeneous, while the microstructure of mixed gels appear to be coarse. The microstructure of SPI-gum mixed gels results from the competition between gelation of the protein aggregates and the phase separation between protein aggregates and polysaccharide molecules (Jong, Klok & van de Velde, 2009). At first, the solution starts to phase separate into protein and serum phase due to the size incompatibility between the protein and the polysaccharide. Subsequently as the pH decreased toward the isoelectric point of SPI, the solution starts to gel (van den Berg et al., 2009). Fig. 6. showed that the area covered by the gum in these gels (where protein is main fraction) increased with the increase in gum (XG, GG) concentration. This aspect is much more evident in the case of SPI-GG mixed gels. The difference in the microstructure in SPI-XG and SPI-GG mixed gels can be attributed to the charge density of XG (0.25 mol negative charge/mol of monosaccharide) and GG (uncharged polysaccharide) (de Jong & van de Velde, 2007). The charge density of polysaccharides is the most dominating factor in the formation of microstructure. The charged polysaccharide (XG) gets distributed in more dispersed manner compared to the uncharged polysaccharide (GG) due to the electrostatic repulsion.

The increase in the proportion occupied by GG in SPI-GG mixed gels also indicates that an increase of GG concentration from 0.05% to 0.3% (w/w) increased the density of protein aggregates in the protein continuous part which enhanced their elastic response (Rocha, Teixeira, Hilliou, Sampaio & Gonçalves, 2009). These changes in microstructure of SPI-GG mixed gels are in accordance with rheological properties of mixed gels (Section 3.2.1) above. The proportion occupied by XG also becomes more and more prominent in the case of SPI-XG mixed gels when the concentration of XG increased.

4. Conclusions

The effect of addition of xanthan gum (XG) and guar gum (GG) on the rheological properties and microstructure of glucono-δ-lactone induced SPI-gum (XG, GG) gels were investigated. The apparent shear viscosity of all mixed solutions increased with the increase in both SPI and gum (XG, GG) concentration. All these mixed solutions showed a shear-thinning behavior. The addition of even very small amount of gum (XG, GG) significantly increased both the storage (G') and loss (G'') moduli for SPI-gum (XG, GG) mixed gels compared to those of SPI only gels. G' and G'' of the mixed gels increased with increase in the angular frequency. The Burger model fitted the creep recovery data reasonably well ($R^2 > 0.919$) and this model showed that instantaneous elastic strain in these mixed gels was larger than the retarded elastic and viscous flow deformation. The proportion occupied by gum in mixed gels was found to increase with the increase in the concentration of gums which increased the density of protein aggregates in the mixed gels.

Acknowledgments

This research was supported by Science and Technology Support Project of China (2013BAD10B03), High Technology Research and Development Program of China (2011AA100802), National Natural Science Foundation of China (31000813), Chinese Universities Scientific Fund (2012YJ092, 2012QJ009, 2013YJ007), Commonweal Guild Agricultural Scientific Research Program of China (201003077), and Beijing Municipal Science and Technology Commission Project (Z121100001312010, D12110003112002).

References

Ai-min, S., Wang, L., Li, D., & Adhikari, B. (2012). Suspensions of vacuum-freeze dried starch nanoparticles: influence of NaCl on their rheologial properties. *Journal of Food Engineering*, *113*(1), 61–68.

Alvarez, M. D., Fernández, C., Olivares, M. D., & Canet, W. (2012). A rheological characterisation of mashed potatoes enriched with soy protein isolate. *Food Chemistry*, *133*(4), 1274–1282.

Andrew, T. R. (1977). *Applications of xanthan gum in foods and related products. Extracellular microbial polysaccharides*. Washington, DC: American Chemical Society.

Bi, C., Li, D., Wang, L., Wang, Y., & Adhikari, B. (2013). Characterization of non-linear rheological behavior of SPI–FG dispersions using LAOS tests and FT rheology. *Carbohydrate Polymers*, *92*(2), 1151–1158.

Bi, C., Li, D., Wang, L., & Adhikari, B. (2013). Viscoelastic properties and fractal analysis of acid-induced SPI gels at different ionic strength. *Carbohydrate Polymers*, *92*(1), 98–105.

Cavallieri, A. L. F., & Da Cunha, R. L. (2008). The effects of acidification rate, pH and ageing time on the acidic cold set gelation of whey proteins. *Food Hydrocolloids*, *22*(3), 439–448.

Chagas, B. S., Machado, D. L. P., Haag, R. B., De Souza, C. R., & Lucas, E. F. (2004). Evaluation of hydrophobically associated polyacrylamide-containing aqueous fluids and their potential use in petroleum recovery. *Journal of Applied Polymer Science*, *91*(6), 3686–3692.

Corredig, M., Sharafbafi, N., & Kristo, E. (2011). Polysaccharide–protein interactions in dairy matrices, control and design of structures. *Food Hydrocolloids*, *25*(8), 1833–1841.

de Jong, S., Klok, H. J., & van de Velde, F. (2009). The mechanism behind microstructure formation in mixed whey protein–polysaccharide cold-set gels. *Food Hydrocolloids*, *23*(3), 755–764.

de Jong, S., & van de Velde, F. (2007). Charge density of polysaccharide controls microstructure and large deformation properties of mixed gels. *Food Hydrocolloids*, *21*(7), 1172–1187.

de Kruif, C. G., & Tuinier, R. (2001). Polysaccharide protein interactions. *Food Hydrocolloids*, *15*(4–6), 555–563.

Joshi, M., Aldred, P., Panozzo, J. F., Kasapis, S., & Adhikari, B. (2014). Rheological and microstructural characteristics of lentil starch–lentil protein composite pastes and gels. *Food Hydrocolloids*, *35*, 226–237.

Kasran, M., Cui, S. W., & Goff, H. D. (2013). Emulsifying properties of soy whey protein isolate–fenugreek gum conjugates in oil-in-water emulsion model system. *Food Hydrocolloids*, *30*(2), 691–697.

Morr, C. V. (1990). Current status of soy protein functionality in food systems. *Journal of the American Oil Chemists' Society*, *67*(5), 265–271.

Oh, M., So, J., & Yang, S. (1999). Rheological evidence for the silica-mediated gelation of xanthan gum. *Journal of Colloid and Interface Science*, *216*(2), 320–328.

Özkan, N., Xin, H., & Chen, X. D. (2002). Application of a depth sensing indentation hardness test to evaluate the mechanical properties of food materials. *Journal of Food Science*, *67*(5), 1814–1820.

Perez, A. A., Carrara, C. R., Sánchez, C. C., Santiago, L. G., & Rodríguez Patino, J. M. (2009). Interfacial dynamic properties of whey protein concentrate/polysaccharide mixtures at neutral pH. *Food Hydrocolloids*, *23*(5), 1253–1262.

Petruccelli, S., & Anon, M. C. (1995). Soy protein isolate components and their interactions. *Journal of Agricultural and Food Chemistry*, *43*(7), 1762–1767.

Roberts, K. T. (2011). The physiological and rheological effects of foods supplemented with guar gum. *Food Research International*, *44*(5), 1109–1114.

Rocha, C., Teixeira, J. A., Hilliou, L., Sampaio, P., & Gonçalves, M. P. (2009). Rheological and structural characterization of gels from whey protein hydrolysates/locust bean gum mixed systems. *Food Hydrocolloids*, *23*(7), 1734–1745.

Steffe, J. F. (1996). *Rheological methods in food process engineering*. East Lansing: Freeman Press.

van den Berg, L., Rosenberg, Y., van Boekel, M. A. J. S., Rosenberg, M., & van de Velde, F. (2009). Microstructural features of composite whey protein/polysaccharide gels characterized at different length scales. *Food Hydrocolloids*, *23*(5), 1288–1298.

Wang, Y., Li, D., Wang, L., & Adhikari, B. (2011). The effect of addition of flaxseed gum on the emulsion properties of soybean protein isolate (SPI). *Journal of Food Engineering*, *104*(1), 56–62.

Wang, Y., Wang, L., Li, D., Xue, J., & Mao, Z. (2009). Effects of drying methods on rheological properties of flaxseed gum. *Carbohydrate Polymers*, *78*(2), 213–219.

Whitcomb, P. J., EK, B. J., & Macosko, C. W. (1977). *Rheology of xanthan gum solutions. Extracellular microbial polysaccharides*. Washington, DC: American Chemical Society.

Wong, P. Y. Y., & Kitts, D. D. (2003). A comparison of the buttermilk solids functional properties to nonfat dried milk, soy protein isolate, dried egg white, and egg yolk powders. *Journal of Dairy Science*, *86*(3), 746–754.

Wu, M., Li, D., Wang, L., Özkan, N., & Mao, Z. (2010). Rheological properties of extruded dispersions of flaxseed–maize blend. *Journal of Food Engineering*, *98*(4), 480–491.

Xu, L., Xu, G., Liu, T., Chen, Y., & Gong, H. (2013). The comparison of rheological properties of aqueous welan gum and xanthan gum solutions. *Carbohydrate Polymers*, *92*(1), 516–522.

Ye, A., Hemar, Y., & Singh, H. (2004). Influence of polysaccharides on the rate of coalescence in oil-in-water emulsions formed with highly hydrolyzed whey proteins. *Journal of Agricultural and Food Chemistry*, *52*(17), 5491–5498.

Zhu, J., Yang, X., Ahmad, I., Li, L., Wang, X., & Liu, C. (2008). Rheological properties of κ-carrageenan and soybean glycinin mixed gels. *Food Research International*, *41*(3), 219–228.